World Academy of Science, Engineering and Technology
International Journal of Mechanical and Mechatronics Engineering
Vol:11, No:5, 2017

Effect of Atmospheric Pressure on the Flow at the Outlet of a Propellant Nozzle

R. Haoui

Abstract**—**The purpose of this work is to simulate the flow at the exit of Vulcan 1 engine of European launcher Ariane 5. The geometry of the propellant nozzle is already determined using the characteristics method. The pressure in the outlet section of the nozzle is less than atmospheric pressure on the ground, causing the existence of oblique and normal shock waves at the exit. During the rise of the launcher, the atmospheric pressure decreases and the shock wave disappears. The code allows the capture of shock wave at exit of nozzle. The numerical technique uses the Flux Vector Splitting method of Van Leer to ensure convergence and avoid the calculation instabilities. The Courant, Friedrichs and Lewy coefficient (CFL) and mesh size level are selected to ensure the numerical convergence. The nonlinear partial derivative equations system which governs this flow is solved by an explicit unsteady numerical scheme by the finite volume method. The accuracy of the solution depends on the size of the mesh and also the step of time used in the discretized equations. We have chosen in this study the mesh that gives us a stationary solution with good accuracy.

Keywords**—**Launchers, supersonic flow, finite volume, nozzles, shock wave.

I. Introduction

THE study of propellant thrusters launcher holds great interest in ballistics. The choice of the profile of the convergent of the nozzle is such that the thrust is high at the outlet. The excessive length of this type of nozzles obtained by the characteristic method (9 m) are used as a truncated nozzle, and we take the third of the length from the throat (3 m) [1]. This nozzle is called truncated ideal contour (TIC). In an earlier work, it is already found the truncated ideal profile of this type of propellant nozzle [1]. It is this profile that will be used to simulate the flow at the outlet of the nozzle opening into the atmosphere. For this purpose, a finite volume methodology is employed to determine the flow parameters inside and outside of nozzle. The technology uses the numerical Flux Vector Splitting method of Van Leer. Here, adequate time stepping parameter, along with CFL coefficient and mesh size level are selected to ensure numerical convergence, sought with an order of 10^{-6}. The mesh is divided into two parts, a mesh in the nozzle and the outer mesh of the nozzle. The volume of the atmosphere of the mesh is selected so that one will not have the end effects. In this work, we will test our calculation code using only the Euler equations before taking into account the flow and cryogenic LH_2 and LOX.

R. Haoui is with the Thermo-Energetic Department, University of Sciences and Technology Houari Boumediene, BP32, Al Alia, Algiers, Algeria (e-mail: haoui_rabah@yahoo.fr).

II. Governing Equations

We tested the profile found by the characteristics method with our computer code by using the finite volume method [1], [4] in order to determine the flow parameters in the nozzle which starts by a convergent followed by an arc of circle to the throat. The convergent is connected to the divergent profile found by the characteristics method. The grid used is represented on Fig. 1.

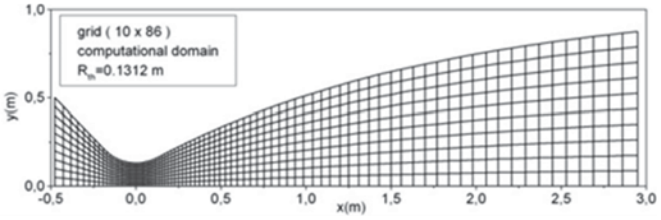

Fig. 1 Computational grid

The profile of the proposed divergent is given by [1]:

$$\frac{y}{R_{th}} = y_1 + A_1.\exp\left[-\frac{\left(\frac{x}{R_{th}}-x_1\right)}{t_1}\right] \quad (1)$$

$$0.943 \leq \frac{x}{R_{th}} \leq 22.8\,; \quad R_{th} = 0.13m \quad (2)$$

with:

$$y_1 = 8.77;\ A_1 = -7.90;\ x_1 = 0;\ t_1 = 17.158 \quad (3)$$

The results are function of grid size, number of iterations and the CFL [2]. The profile is tested and gave the same result with the method of characteristics [1] (Fig. 2).

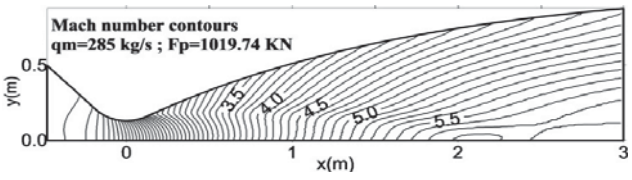

Fig. 2 Mach number contours in the nozzle

We added to the propellant nozzle part of the downstream atmosphere to simulate the flow in function of the variation of the atmospheric pressure. We chose the mesh (n_i, n_j) according to Fig. 3 for such simulation.

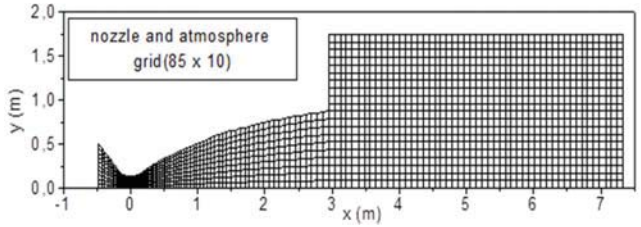

Fig. 3 Computational grid for $P_a = 1\ bar$

The Euler equations in a flux-vector formulation in Cartesian coordinate system are given as [8]-[10].

$$\frac{\partial W}{\partial t} + \frac{\partial E}{\partial x} + \frac{\partial F}{\partial y} + \frac{\partial G}{\partial z} = 0 \tag{4}$$

where W, E, F and G are vectors given by:

$$W = \begin{pmatrix} \rho \\ \rho u \\ \rho v \\ \rho w \\ \rho e \end{pmatrix} \quad E = \begin{pmatrix} \rho u \\ \rho u^2 + p \\ \rho uv \\ \rho uw \\ (\rho e + p)u \end{pmatrix} F = \begin{pmatrix} \rho v \\ \rho uv \\ \rho v^2 + p \\ \rho vw \\ (\rho e + p)v \end{pmatrix} \quad G = \begin{pmatrix} \rho w \\ \rho uw \\ \rho vw \\ \rho w^2 + p \\ (\rho e + p)w \end{pmatrix}$$

The energy per unit of mass e is defined as sum of internal energy and kinetic energy such as:

$$e = c_v T + \frac{1}{2}(u^2 + v^2 + w^2) \tag{5}$$

III. Axisymmetric Formulation

To pass from 3D to 2D axisymmetric problem, we are forced to make changes to a point (x, y, z) to the point (x, r) since the parameters do not change depending on the rotation for a fixed position on the axis of symmetry. The results obtained have shown that the flow is axisymmetric. The system of (4) can be written as [3]:

$$mes(C_{i,j})\frac{\partial W_{i,j}}{\partial t} + \sum_{a\in\{x,x',y,y'\}}(F_{i,j}\vec{i} + G_{i,j}\vec{j}).\overrightarrow{\eta_a} - H.aire(C_{i,j}) = 0 \tag{6}$$

where $mes(C_{i,j})$ is the measurement (in m^3) of an infinitely small volume of center (i, j), $aire(C_{i,j})$ is the surface of the symmetry plane passing by the center of elementary volume and η_a is the integrated normal. The third term of the equation expresses the axisymmetric flow condition. The new Fluxes W, F, G and H becomes [3]:

$$W = \begin{pmatrix} \rho \\ \rho u \\ \rho v \\ \rho e \\ \rho_s \\ (\rho_s e_{vs})_{O2,N2} \end{pmatrix} F = \begin{pmatrix} \rho u \\ \rho u^2 + p \\ \rho uv \\ (\rho e + p)u \end{pmatrix} G = \begin{pmatrix} \rho v \\ \rho uv \\ \rho v^2 + p \\ (\rho e + p)v \end{pmatrix} H = \begin{pmatrix} 0 \\ 0 \\ 2p \\ 0 \end{pmatrix}$$

IV. Discretization in Time

The explicit method was used as an approach in time and space. The time step Δt is calculated by:

$$\Delta t_{i,j} = min\left(\frac{\Delta x.CFL}{\|V\| + a}\right) \tag{7}$$

CFL is a stability factor, V is the velocity of the flow, a the speed of sound and Δx is the small length of the mesh at the same point (i, j). At each time step and for each point(i, j), the system of (6) can be written as [5], [11]:

$$W_{i,j}^{n+1} = W_{i,j}^{n} - \frac{\Delta t_{i,j}}{mes(C_{i,j})} \sum_{a\in\{x,x',y,y'\}} (F_{i,j}{}^{n}\vec{i} + G_{i,j}{}^{n}\vec{j})\overrightarrow{\eta_a} + \Delta t_{i,j}\frac{aire(C_{i,j})}{mes(C_{i,j})} H_{i,j}{}^{n} \tag{8}$$

The choice of the grid and CFL plays an important role to obtain the stationary solution [2].

V. Decomposition of Van-Leer

The use of the decomposition of Van Leer is necessary in supersonic flow [4], [12]. We decompose the flux f into two parts f_{VL}^{-} and f_{VL}^{+} such that $f = f_{VL}^{-} + f_{VL}^{+}$. This decomposition is applied through an interface between two nodes. In 2D, we project speeds in the new marker containing the normal to the facet in broken line forming an angle θ compared to the axis of symmetry, rotation R, Fig. 4 [5].

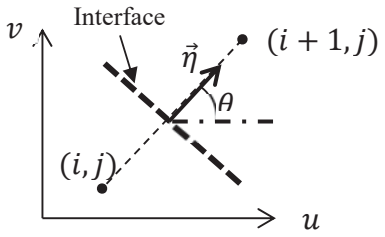

Fig. 4 Interface

The Euler new vector W_E^R is written in the new reference mark as:

$$W_E^R = \begin{pmatrix} \rho \\ \rho\overrightarrow{V_n} \\ \rho\ e \end{pmatrix} \tag{9}$$

where $\overrightarrow{V_n}$ is obtained from $\vec{V}$, via the rotation R, in the following way:

$$\vec{V} = \begin{pmatrix} u \\ v \end{pmatrix} \rightarrow \vec{V}_n = \begin{pmatrix} u_n \\ v_n \end{pmatrix} = \begin{pmatrix} cos\,\theta & sin\,\theta \\ -sin\,\theta & cos\,\theta \end{pmatrix}\begin{pmatrix} u \\ v \end{pmatrix} \tag{10}$$

where

$$cos\,\theta = \frac{\eta_x}{\|\vec{\eta}\|}, \quad sin\,\theta = \frac{\eta_y}{\|\vec{\eta}\|} \tag{11}$$

$$\|\vec{\eta}\| = \sqrt{\eta_x^2 + \eta_y^2} \tag{12}$$

The overall transformation R is written overall:

$$R = \begin{pmatrix} cos\,\theta & sin\,\theta \\ -sin\,\theta & cos\,\theta \end{pmatrix} \tag{13}$$

$$R^{-1} = \begin{pmatrix} cos\,\theta & -sin\,\theta \\ sin\,\theta & cos\,\theta \end{pmatrix} \tag{14}$$

Moreover, at each interface $i+1/2$, two neighbor states i and $i+1$ are known, Fig. 4. Thus, we can calculate the one-dimensional flow F through the interface, total flow $f(W,\eta)$ being deduced from F by applying the opposite rotation, as:

$$f(W,\vec{\eta}) = \|\vec{\eta}\|.R^{-1}\big(F(W^R)\big) \tag{15}$$

According to Fig. 4, we project the velocities (u,v) on the normal of the facet and we use the component u_n to calculate the flow rate through this facet. One more here will help us to separate the supersonic flow of supersonic flow in order to use the Vann-Leer decomposition. After calculating the flow in the reference of the normal $\vec{\eta}$, we return to the mark (x,r) via the reverse rotation to determine all parameters of flow. The expression of Van-Leer decomposition is as:

$$F_{VL}^{+}(W^R) = \begin{cases} F(W^R) & M_n \geq 1 \\ \begin{pmatrix} \frac{\rho a}{4}\left(\frac{u_n}{a}+1\right)^2 = f_1^{+} \\ \frac{f_1^{+}}{\gamma}[(\gamma-1)u_n+2a] \\ f_1^{+}.v_n \\ \frac{f_1^{+}}{2}\left[\frac{((\gamma-1)u_n+2a)^2}{\gamma^2-1}+v_n^2\right] \end{pmatrix} & |M_n|<1 \\ 0 & M_n \leq -1 \end{cases} \tag{16}$$

$$F_{VL}^{-}(W^R) = \begin{cases} 0 & M_n \geq 1 \\ \begin{pmatrix} \frac{\rho a}{4}\left(\frac{u_n}{a}-1\right)^2 = f_1^{-} \\ \frac{f_1^{-}}{\gamma}[(\gamma-1)u_n-2a] \\ f_1^{-}.v_n \\ \frac{f_1^{-}}{2}\left[\frac{((\gamma-1)u_n-2a)^2}{\gamma^2-1}+v_n^2\right] \end{pmatrix} & |M_n|<1 \\ F(W^R)M_n & \leq -1 \end{cases} \tag{17}$$

where $M_n = u_n/a$, u_n and v_n are the normal and tangential velocities to the $\vec{\eta}$ respectively.

VI. Boundary Conditions

In unsteady problems, the initial values of all flow variables need to be specified at all points in the computational domain. The present work describes the implementation of the following most common boundary conditions in the discredited equations of the finite volume method: inlet, outlet, wall and symmetry [5], [6].

A. Inlet

At the nozzle inlet the pressure and temperature are fixed, but the law rate of the flow, M=0.019, obligate us to leave floating one of flow parameters. Here, one chooses to extrapolate the module of velocity from the interior of the solution domain. This correction allows an adjustment of the flow rate.

B. Body Surface

In this case, as flow is not viscous, a slip condition is applied on the wall. At any point on the wall the following condition must be checked:

$$\vec{V}.\vec{n} = 0 \tag{18}$$

$\vec{n}$ is the normal to the wall.

C. Axis of Symmetry

The conditions at axis of symmetry boundary are no flow and no scalar flux across the axis.

D. Outlet

At the exit of the computational domain, the pressure is fixed, the values of others flow parameters are extrapolated from the interior values. Three grids were tested for the nozzle, $(256x30)$, $(341x40)$ and $(426x50)$. For the downstream reservoir the grid is $(5n_j, 2n_j)$. From the last mesh, results are unchanged and the residue is about 10^{-6}.

VII. Results and Interpretations

Let's start with the numerical simulation with a downstream pressure $Pa = 1\ bars$ (Fig. 5). The flow is supersonic at the exit of the nozzle with the existence of an oblique shock wave attached to the wall [7], and a normal shock at the center of nozzle, called Mach disk. It is understood that in reality the oblique shock is slightly advanced in the divergent because of the turbulence. Floor nozzle is over expanded regime. The presence of the right shock at the center of the flow is to cause the pressure on the axis at the outlet of the nozzle is smaller than the wall. More atmospheric pressure decreases during the rise of the pitcher over the output shock waves will be less intense until arriving at the event tailored to approximately 15 to 20 km altitude, and after this, the regime of the nozzle becomes under expanded. Take the case that comes to 6 km altitude where the atmospheric pressure is 0.5 bar, shock waves at the exit of the nozzle is less intense (Fig. 6). In the case where the atmospheric pressure is 0.08 bar, which corresponds to an altitude of 17 km, the flow is without the presence of shock waves and the nozzle is adapted regime (Fig. 7), the fluid streams diverging near the wall as the output pressure is greater than 0.08 bar and near the axis the flow converges because the output pressure is lower than 0.08 bar. For more than 20 km altitude, the jet at the outlet of the propelling nozzle is diverges, Fig. 8 shows the case where the atmospheric pressure is $0.02bar$. The grid of the reservoir is $(5n_j, 3n_j)$. Note that while climbing the V_a speed outside air over the vehicle does not affect the flow behavior outside except with a little closer to the axis of symmetry (Fig. 9).

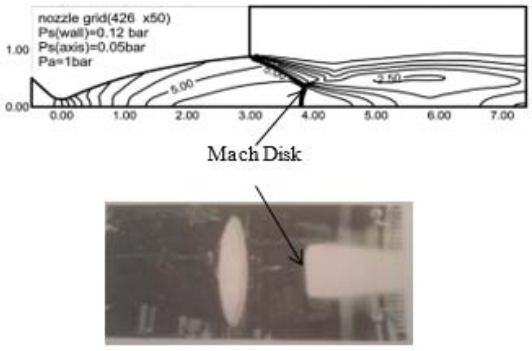

Fig. 5 Configuration for $P_a = 1\ bar$

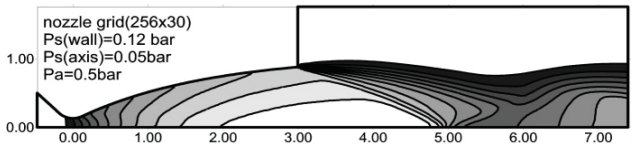

Fig. 6 Configuration for $P_a = 0.5\ bar$

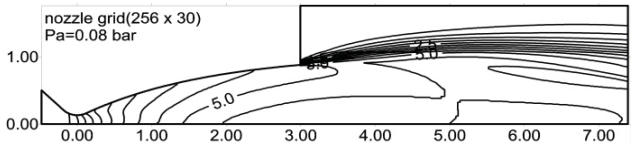

Fig. 7 Configuration for $P_a = 0.08\ bar$

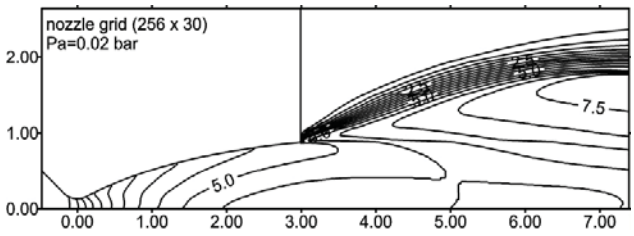

Fig. 8 Configuration for $P_a = 0.02\ bar$

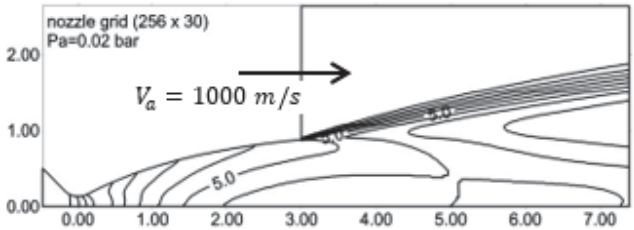

Fig. 9 Configuration for $P_a = 0.02\ bar$ with exit flow

VIII. Conclusion

In conclusion, the flow at the outlet nozzles propellant is done with the existence of oblique shock waves relating to the wall and a normal shock at the center. This occurs only at the beginning of the rise of the launcher. In most of the trip operation is done without shock waves. The only way for the moment, to get rid of this, is to increase the pressure in the combustion chamber, this course requires stronger materials.

References

[1] Haoui, R., "Design of the propelling nozzles for the launchers and satellites", International Journal of Aeronautical and space Sciences, 15(1), 2014, pp91-96. DOI:10.5139/IJASS.2014.15.1.91.

[2] Haoui, R. Gahmousse, A. Zeitoun, D., "Condition of convergence applied to an axisymmetric reactive flow", 16th CFM, n°738, Nice, France, 2003.

[3] Goudjo, J.A. Désidéri, "A finite volume scheme to resolution an axisymmetric Euler equations (Un schéma de volumes finis décentré pour la résolution des équations d'Euler en axisymétrique)," Research report INRIA 1005, 1989.

[4] Van Leer, B., "Flux Vector Splitting for the Euler Equations", Lecture Notes in Physics. 170, 1982, 507-512.

[5] Haoui, R., "Finite volumes analysis of a supersonic non-equilibrium flow around the axisymmetric blunt body", International Journal of Aeronautical and space Sciences, 11(2), 2010, pp59-68. DOI:10.5139/IJASS.2010.33.1.059

[6] Haoui, R., "Effect of Mesh Size on the Viscous Flow Parameters of an Axisymmetric Nozzle", International Journal of Aeronautical and space Sciences, 12(2), 2011,

[7] Shapiro, A.H. (1954). The Dynamics and Thermodynamics of Compressible fluid flow. The Ronald Press Company, New York. Volume II. Ch.17.

[8] H. Schlichting, Boundary-layer theory, 7th edition, McGraw-Hill, New York, 1979.

[9] K. A. Hoffmann, Computational fluid dynamics for engineers, Volume II. Chapter 14, Engineering Education system, Wichita, USA, pp.202-235, 1995.

[10] Joel H. Ferziger & M. Peric, Computational Methods for Fluid Dynamics, Chapter 8, Springer-Verlag, Berlin Heidelberg, New York, 2002, pp.217-259,

[11] M-C. Druguet, "Contribution to the study of nonequilibrium reactive hypersonic Euler's flows," Thesis of Doctorate. University of Provence, France, 1992.

[12] L. Landau, E. Teller, "Theory of sound dispersion," Physikalische Zeitschrift der Sowjetunion. 10, (1936), 34-43.